

Article

Three Technical Challenges Faced by Power Systems in Transition

Zheng Xu 

Department of Electrical Engineering, Zhejiang University, Hangzhou 310027, China; xuzheng007@zju.edu.cn

Abstract: In the 21st century, the worldwide concern about global warming has forced energy to transform in the direction of low-carbon and non-carbon. The utilization of renewable energy is developing rapidly, which makes the non-synchronous generator sources become the main part of the newly added power sources. Based on the fundamentals of AC power grid operation, this paper describes three technical challenges faced by the power system in transition: the inadequacy of the classic synchronization stability concept in representing the new synchronization connotation of AC power systems with large proportion of non-synchronous generator sources; the inapplicability of the electromechanical transient analysis method in analyzing the generalized synchronization stability; and the wideband resonance instability caused by negative resistance of power electronic equipment. The decisive factors for maintaining the generalized synchronization stability, the countermeasure to solve the inapplicability of the electromechanical transient analysis method and a systematic approach to tackle the broadband resonance instability are proposed in the paper.

Keywords: non-synchronous generator source; generalized synchronization stability; phase locked loop; power synchronization loop; failure of phase locking; time delay out-of-step; electromechanical transient analysis; electromagnetic transient analysis; broadband resonance stability; s-domain nodal admittance matrix



Citation: Xu, Z. Three Technical Challenges Faced by Power Systems in Transition. *Energies* **2022**, *15*, 4473. <https://doi.org/10.3390/en15124473>

Academic Editor: Abu-Siada Ahmed

Received: 14 May 2022

Accepted: 16 June 2022

Published: 19 June 2022

Publisher's Note: MDPI stays neutral with regard to jurisdictional claims in published maps and institutional affiliations.



Copyright: © 2022 by the author. Licensee MDPI, Basel, Switzerland. This article is an open access article distributed under the terms and conditions of the Creative Commons Attribution (CC BY) license (<https://creativecommons.org/licenses/by/4.0/>).

1. Introduction

With the continuous development of energy transformation, the proportion of fossil energy will continue to decline, and the proportion of renewable energy, especially solar energy and wind energy, will continue to increase [1,2]. In addition to the uncontrollability and volatility, solar and wind power generation based on the mainstream technology is different from fossil power generation in that it belongs to non-synchronous generator sources [3–5]. The uncontrollability and volatility of solar and wind power generation poses a great challenge to the power and energy balance of large-scale power grids, which requires the use of power and energy balance methods different from the traditional methods, such as energy storage, active response on the load side, etc. [6–8]; furthermore, the non-synchronous generator characteristics of solar and wind power pose a major challenge to the synchronization stability theory of large power grids. With a large number of non-synchronous generator sources entering the power grid, the dominant position of synchronous generator sources in the power grid is overturned, resulting in essential changes in the operation characteristics of the power system [9,10]. The grid with high proportion of non-synchronous generator sources will face three technical challenges:

- (1) the inadequacy of the classic synchronization stability concept in representing the new synchronization connotation of AC power systems, which should be extended to the generalized synchronization stability;
- (2) the inapplicability of the electromechanical transient analysis method in analyzing the generalized synchronization stability;
- (3) the instability of broadband resonance caused by negative resistance of power electronic equipment.

This paper is organized as follows. Section 2 describes the new connotation of synchronization stability—the generalized synchronization stability. Section 3 discusses the basic means to keep the generalized synchronization stability for non-synchronous generator sources. Section 4 gives the difference of the synchronization mechanism between the synchronous generator and the non-synchronous generator sources. Section 5 describes the three types of out-of-step of the generalized synchronization stability. Section 6 discusses the inapplicability of the electromechanical transient analysis method in analyzing the generalized synchronization stability, and the substitution use of the electromagnetic transient analysis method is proposed. Section 7 discusses the analysis method of the broadband resonance instability caused by negative resistance of power electronic devices. Section 8 gives the summary of the paper.

2. The New Connotation of Synchronization Stability—The Generalized Synchronization Stability

The characteristics of the AC power grid require that all power sources must be of the same frequency. If one power source is of different frequency, the source must be cut off, otherwise the whole AC power grid cannot operate; that is, the necessary condition for operating an AC power grid is that all power sources in the grid must be of the same frequency. In an AC power grid dominated by synchronous generators, the ability to keep all synchronous generators at the same frequency is called the synchronization stability, which is also presented as the power angle stability between synchronous generators [11].

In an AC power grid with synchronous generator and non-synchronous generator sources coexisting, keeping all power sources at the same frequency is still a necessary condition for operating the AC power grid. However, its implication is different from that of the AC power grid dominated only by synchronous generators. The power angle stability between synchronous generators is not enough to ensure that the synchronous generators and non-synchronous generator sources are of the same frequency. Since the non-synchronous generator source is generally controlled by power electronic converters, its ability to maintain synchronization with other power sources in the grid is not its inherent characteristic, but a characteristic that must be realized by the controller. This is essentially different from the synchronous generator.

Thus, in an AC power grid where synchronous generators and non-synchronous generator sources coexist, the concept of synchronization stability in an AC power grid dominated only by synchronous generators, must be extended theoretically to include the same frequency operating condition among all the power sources with different synchronization mechanisms. We define the condition that all power sources in an AC power grid maintain operating in the same frequency as the generalized synchronization stability [12,13], as shown in Figure 1. In this way, the generalized synchronization stability includes the following three aspects: (1) the synchronization stability among the traditional synchronous generators; (2) the synchronization stability among the synchronous generators and the non-synchronous generator sources; (3) the synchronization stability among the non-synchronous generator sources.

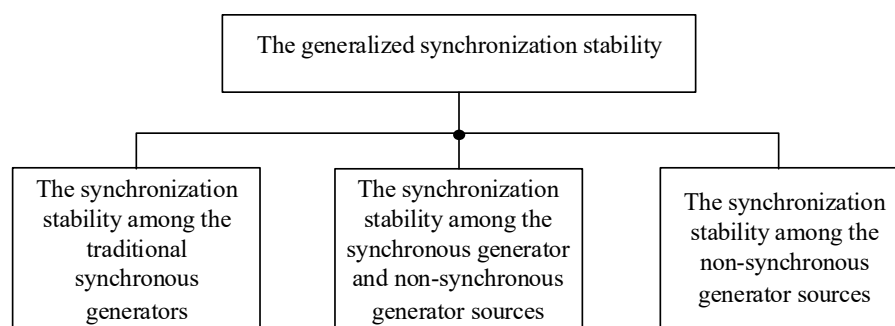


Figure 1. The implication of the generalized synchronization stability.

3. The Basic Means of Keeping Generalized Synchronization Stability for Non-Synchronous Generator Sources

The typical structure of a non-synchronous generator source is shown in Figure 2, which is actually a converter. In Figure 2, the valve side voltage and the grid side voltage of the voltage source converter (VSC) are u_v and u_s respectively, the amplitude and the angular frequency of u_s are U_s and ω respectively, t is the time in second, and θ equals ωt . Fundamentally, the non-synchronous generator sources can be divided into two types, the grid following converter source and the grid forming converter source [14,15].

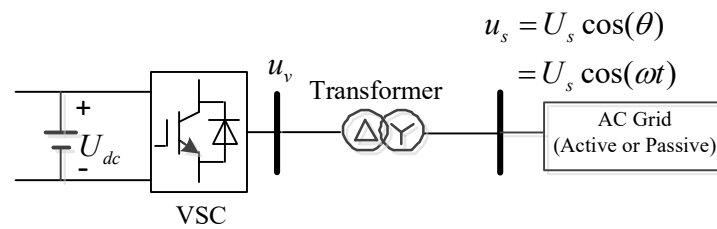


Figure 2. Typical structure of a non-synchronous generator source.

The external characteristic of the grid following converter source is of the current source [16], and it must be connected to an active grid. The control strategy of the grid following converter source is to control the amplitude and phase angle of the current injected to the grid by the converter. The grid following converter source can be a voltage source converter or a current source converter; the typical representatives are the traditional line commutation converter (LCC) [17], the doubly fed induction generator (DIFG) [18] and the voltage source converter with AC current direct control [16].

For the grid following converter source, the basic means to keep synchronization with the grid power source is to use the phase-locked loop (PLL) to track the phase angle of its grid side voltage u_s . Figure 3 shows the schematic diagram of a PLL based on the synchronous reference frame (SRF-PLL) [16].

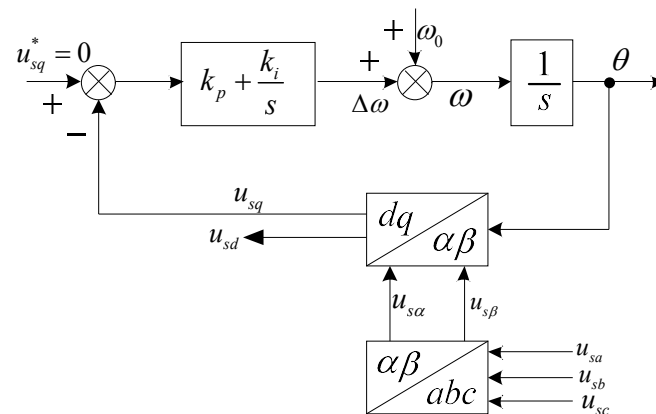


Figure 3. Principle block diagram of SRF-PLL based on control theory.

In the principle shown in Figure 3, the problem of phase-locked synchronization is treated as an automatic control problem, that is, to control the output θ of the SRF-PLL to maintain $u_{sq} = 0$. In Figure 3, u_{sa}, u_{sb}, u_{sc} are the instantaneous three-phase grid side voltage of the VSC in Figure 2; $u_{s\alpha}, u_{s\beta}$ are the output of the Clarke Transform ($\alpha\beta$ Transform) of u_{sa}, u_{sb}, u_{sc} ; u_{sd}, u_{sq} are the output of the Park Transform (dq Transform) of $u_{s\alpha}, u_{s\beta}$; k_p, k_i are the coefficients of the PI controller; ω_0 is the rated grid angular frequency; and the superscript * means reference value. For the SRF-PLL, the main parameters that determine the performance of the SRF-PLL are mainly the PI controller parameters, the detail operation principle of PLL can be found in [19–24]. When the PLL loses stability, it means a failure of phase-locking occurs, and a failure of phase-locking means that the

synchronization stability between the non-synchronous generator source and the grid power source is lost, whose appearance is out-of-step oscillation.

The external characteristic of the grid forming converter source is of the voltage source, and it can be connected to a passive grid as a supporting source. Note that not all converters can become grid forming converter sources. One of the basic conditions for becoming a grid forming converter source is that the DC side voltage U_{dc} of the converter in Figure 2 must be able to maintain constant by other converters or by energy storage devices. The total two control degrees of freedom of the VSC in Figure 2 are used to control the amplitude U_s and phase angle θ of the grid side voltage u_s , under the condition that the DC side voltage U_{dc} can be maintained constant by the external circuit.

There are two basic means to keep the grid forming converter source synchronized with the grid power source. One method is to use PLL to track the phase angle θ of the grid side voltage u_s , or directly give the phase angle θ when it is used as the supporting source of a passive network [16]; the other is to use power synchronization control (PSC) based on the power synchronization loop (PSL) [25] or virtual synchronous generator (VSG) control [26,27] to maintain synchronization with the grid power source.

For the non-synchronous generator source which uses the PLL to keep synchronization with the grid power source, the key factor of losing generalized synchronization stability is the failure of phase locking.

For the non-synchronous generator source which uses the PSL to keep synchronization with the grid power source, the key factor of losing generalized synchronization stability is the out-of-step of the PSL. The structure of the PSL is shown in Figure 4 [16], which simulates the motion equation of the synchronous generator:

$$2H \frac{d\Delta\omega}{dt} = P_m - P_e - D\Delta\omega \tag{1}$$

$$\frac{d\theta}{dt} = \omega \cdot \omega_0 \tag{2}$$

where, H is the inertia time constant of the generator in second; $\Delta\omega = \omega - \omega_0$ is the generator speed deviation, ω is the actual speed in pu, ω_0 is the rated speed in pu; t is the time in second; P_m is the mechanical power in pu; P_e is the electromagnetic power in pu; D is the damping coefficient in pu; θ is the generator rotor electrical angle in radian.

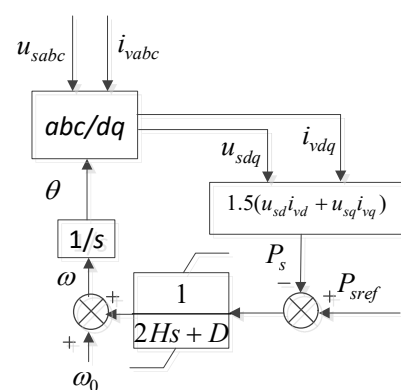


Figure 4. Block diagram of power synchronization loop PSL.

In Figure 4, u_{sabc} and i_{vabc} are the instantaneous three-phase grid side voltage and instantaneous three-phase valve side current of the VSC in Figure 2 respectively; u_{sdq} and i_{vdq} are the output of abc to dq transform of u_{sabc} and i_{vabc} respectively; P_{sref} and P_s are the reference value and the actual value of the active power injected into the AC system by the non-synchronous generator source respectively. The control block diagram of the PSL shown in Figure 4 is obtained by replacing the mechanical power P_m with P_{sref} and electromagnetic power P_e with P_s in Equation (1).

4. The Difference in Synchronization Mechanism between Synchronous Generators and Non-Synchronous Generator Sources

The synchronization mechanism of synchronous generators is determined by three kinds of equations.

- The first kind of equations is the rotor motion equation (also known as swing equation) in (1) and (2), which describes the relationship between the rotor motion (represented by the rotor angle relative to a reference coordinate system) and mechanical power and electromagnetic power;
- the second kind of equations is the mechanical power equation describing the characteristic of the mechanical power, which is mainly determined by the characteristics of the speed regulator of the generator;
- the third kind of equations is the electromagnetic power equation of the generator which describes the relationship between the output electromagnetic power of the generator and the voltage magnitudes and phase angles of other synchronous generators (equivalent electromotive force is used in the generators) in the grid.

The external performance of the synchronization mechanism of the synchronous generators is mainly reflected in the three-stage response characteristics of synchronous generators after grid disturbances. For example, when a synchronous generator in the power grid is suddenly cut off, all the other synchronous generators in the power grid will participate in the compensation of the missing power; however, due to the unique synchronization mechanism of the synchronous generators, the distribution pattern of the compensation power in all synchronous generators varies with the different time stages after the disturbance [28].

- In the first stage after the disturbance, the compensation power provided by each synchronous generator comes from the magnetic field energy of the generator, which is distributed according to the synchronous power coefficient between each synchronous generator and the tripped generator; the larger the synchronous power coefficient is, the greater the compensation power is allocated; if the synchronous power coefficient is negative, the compensation power allocated is also negative.
- In the second stage after the disturbance, the speed change rate of all synchronous generators tends to be the same. The compensation power provided by each synchronous generator comes from the rotor kinetic energy, which will be distributed according to the inertia constant of each synchronous generator.
- In the third stage after the disturbance, the speed of all synchronous generators tends to be the same, and the compensation power provided by each synchronous generator comes from the output power of the prime mover changed by the governor action, which is distributed according to the reciprocal value of the governor's droop coefficient.

There are many types of non-synchronous generator sources. Taking a typical voltage source converter as an example, two equations are decisive to determine its synchronization mechanism.

- The first equation is the AC side output equation of the converter, which is determined by the AC side control objectives of the converter itself.
- The second equation is an equation describing how to obtain the synchronization signal; and if the PLL is used, it is the equation of the PLL, and if the PSL is used, it is the equation of the PSL.

The dynamic equation of the PLL can be derived from Figure 3, and its dynamic characteristics have been studied [29,30]. The dynamic equation of the PSL imitates the equation of the synchronous generator [16,26,27], so its external response characteristics can have some similarities with the synchronous generator. The external performance of non-synchronous generator sources under different synchronization mechanisms is still a subject that needs to be studied.

5. Out-of-Step Types in the Sense of the Generalized Synchronization Stability

According to the current engineering experience, there are two main causes for losing the synchronization stability of non-synchronous generator sources:

- The first is the phase locking failure of the PLL or the out-of-step of the PSL;
- The second is the long delay caused by the accumulation of time delays in each link of the converter control system [31].

In this way, the out-of-step in the sense of the generalized synchronization stability can be divided into three types:

- The power angle instability between the synchronous generators (the power angle out-of-step),
- The phase locking failure of the PLL or the out-of-step of the PSL in the non-synchronous generator sources;
- The out-of-step caused by long time delay of the converter control system in the non-synchronous generator source.

For each of the above types of out-of-step, it can be divided into small disturbance out-of-step and large disturbance out-of-step. In this way, the types of losing the generalized synchronization stability can be summarized as shown in Figure 5.

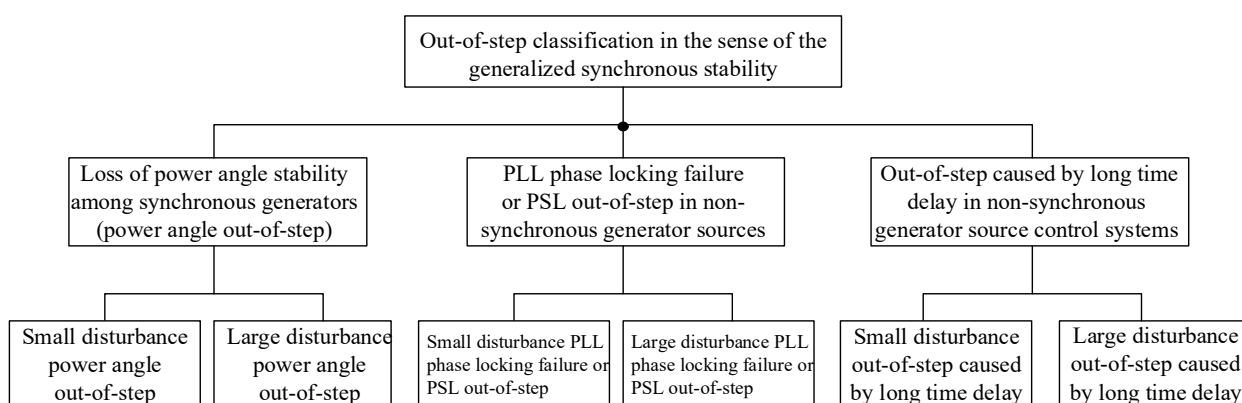


Figure 5. Types of losing the generalized synchronization stability.

It is worth pointing out that the above three types of out-of-step are coupled with each other, that is, the power angle out-of-step between synchronous generators may lead to the phase locking failure of the PLL or out-of-step of the PSL in non-synchronous generator sources; conversely, the phase locking failure of the PLL or out-of-step of the PSL in non-synchronous generator sources may also lead to power angle out-of-step between synchronous generators. Therefore, the three types of out-of-step must be considered simultaneously for the generalized synchronization stability analysis of practical large-scale systems. In this way, the relationship between power angle stability of traditional synchronous generators and the generalized synchronization stability can be represented by Figure 6. The generalized synchronization stability contains the power angle stability. Keeping power angle stability between synchronous generators cannot ensure the generalized synchronization stability of the whole system. In other words, the traditional power angle stability between synchronous generators is only a necessary condition for the whole system to maintain the generalized synchronization stability.

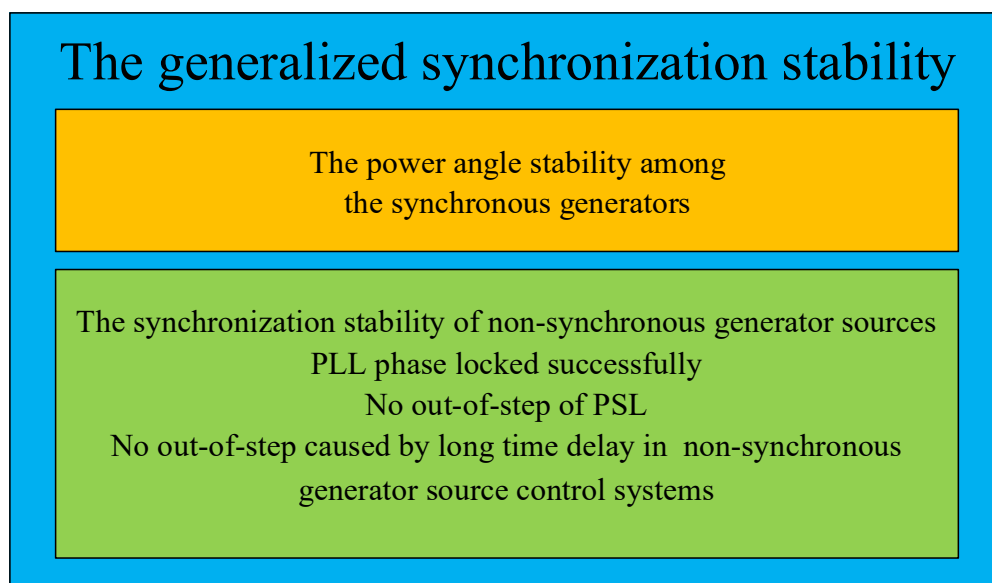


Figure 6. Relationship between the power angle stability and the generalized synchronization stability.

Example to Illustrate the Behaviour under PLL Phase Locking Failure

The study system consists of one generator and one inverter station, supplying power to the load, as shown in Figure 7 [16]. In Figure 7, jx_t represents the equivalent impedance of the generator step-up transformer, $(r_r + jx_r)$ represents the line impedance from the PCC of the inverter station to the load; i_s and u_s are the current and voltage at PCC respectively. Assuming that the generator capacity is 270 MVA; the load active power is 400 MW under the rated voltage with the power factor of 0.95; the power supply proportion of the inverter station is 40%; the inverter station adopts the grid following control and operates in constant active power and constant reactive power mode; the DC side of the inverter is represented by a constant DC voltage source; and the load adopts the constant impedance model. A three-phase short-circuit fault on the load bus (high-voltage side of the step-up transformer) is investigated. It is assumed that the fault occurs in 0.1 s and the fault duration is 0.1 s.

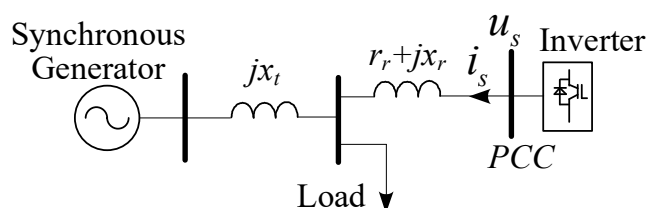


Figure 7. The circuit diagram of the study system.

The time domain simulation results of the main physical quantities are shown in Figure 8 [16]. In Figure 8, i_d and i_q are the d axis component and q axis component of i_s . It can be seen from Figure 8 that after the fault occurs, the generalized synchronization stability between the generator and the inverter is lost because the PLL cannot lock the rotor angle of the synchronous generator, resulting in divergent oscillations of the physical quantity of the system. It has been demonstrated in reference [16] that when the AC system short-circuit ratio of the inverter is less than 1.4, phase locking failure of the PLL is likely to occur.

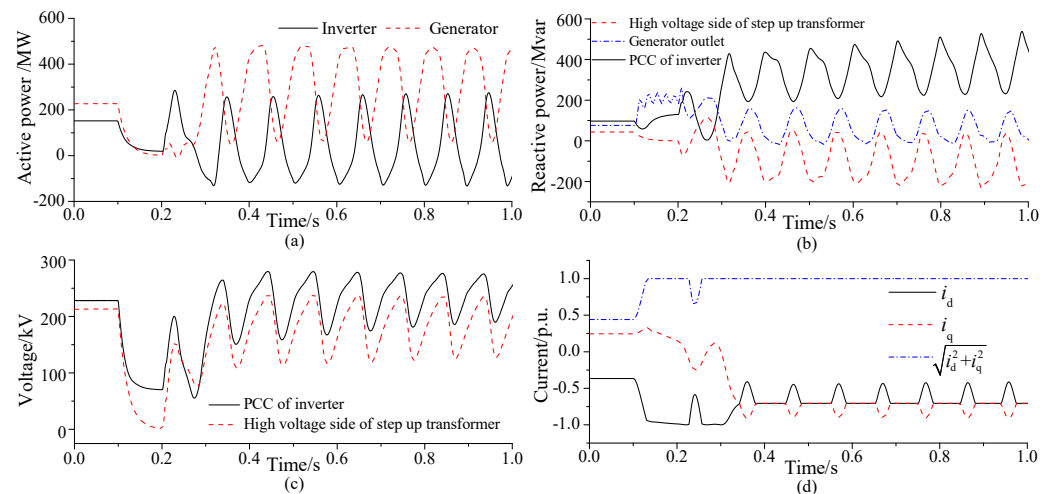


Figure 8. The behaviour under PLL phase locking failure: (a) active power of inverter and generator, (b) reactive power of inverter and generator, (c) voltage of inverter and load, and (d) AC current of inverter.

6. The Inapplicability of Electromechanical Transient Analysis Method and Comprehensive Substitution of Electromagnetic Transient Analysis Method in Analyzing the Generalized Synchronization Stability

Traditionally, the fundamental purpose of electromechanical transient analysis of the power system is to investigate the synchronization stability (also called angle stability) among synchronous generators from the overall level of the power system. The core problem is to study the swing process between generator rotors, and the fundamental factor determining the swing process of the generator rotors is the energy transfer. Therefore, in the electromechanical transient analysis of power systems, the factors that are not closely related to the energy transfer can be ignored. Since the energy transfer in the AC grid mainly depends on the positive sequence fundamental frequency electrical quantities, other non-positive sequence and non-fundamental frequency electrical quantities almost have no impact on the energy transfer (only the positive sequence voltage and current of the same frequency can constitute the average power, thus realizing the energy transfer). Therefore, the AC grid model used for electromechanical transient analysis has the following three characteristics [32]:

- ignoring the electromagnetic transient process in the AC grid, only the fundamental frequency electrical quantity in the AC grid is considered;
- the AC grid is represented by positive sequence fundamental frequency impedance and described by algebraic equations;
- the electrical quantity in the AC grid is represented by a positive sequence fundamental frequency phasor, not an instantaneous value.

The electromechanical transient analysis method widely used in the industry has two limitations when it is used to analyze the generalized synchronization stability of the power systems with large proportion of non-synchronous generator sources.

The first limitation can be seen from Figure 3 or Figure 4. The input of the PLL (or PSL) is the instantaneous value of the converter grid side voltage, but when electromechanical transient analysis method is adopted, only the positive sequence phasor of the converter grid side voltage can be obtained. Therefore, the behavior of the PLL (or PSL) cannot be accurately analyzed by the electromechanical transient analysis method. That is, the positive sequence fundamental frequency phasor model is unable to simulate the behavior of the PLL (or PSL). Thus, the electromechanical transient analysis method is unable to analyze the generalized synchronization stability of the non-synchronous generator sources.

The second limitation is that the fundamental frequency equivalent models of the non-synchronous generator sources and other power electronic equipment can only be obtained

under three-phase symmetry condition. In other words, under asymmetric fault conditions it is difficult to accurately represent the behavior of the power electronic equipment only by the positive sequence fundamental frequency phasors. Simply speaking, to power electronic equipment, there is no mathematical model suitable for electromechanical transient analysis under asymmetric AC system faults.

In this way, the electromechanical transient analysis method can only be used to analyze the power angle stability between synchronous generators under symmetrical fault conditions, and it must be assumed that the performance of PLL or PSL is ideal, that is, the phase locking failure of the PLL and the out-of-step of the PSL cannot be considered. If the scope of the generalized synchronization stability analysis of the power system is represented by the large rectangle area in Figure 9, and the scope of power angle stability analysis between synchronous generators is represented by the small rectangle area in Figure 9, then the scope that can be analyzed by the electromechanical transient analysis method is only the shadow part area in the small rectangle in Figure 9.

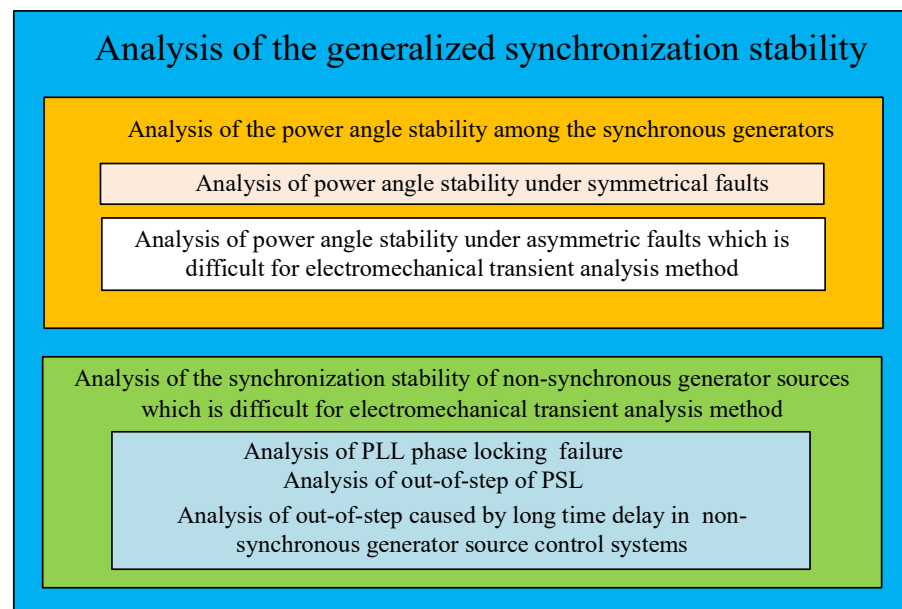


Figure 9. Inclusion relationship between generalized synchronization stability analysis and power angle stability analysis.

From a more macro perspective, for the three major calculations of traditional power systems: the power flow calculation, the short-circuit current calculation and the transient synchronization stability calculation, only the power flow calculation can still be used in its original form for the new power system with large proportion of non-synchronous generator sources. The other two calculations: the short-circuit current calculation and the transient synchronization stability calculation, are no longer applicable to the new power system containing large proportion of non-synchronous generator sources, because in both calculations the behavior of the PLL and the PSL must be simulated accurately, which needs the instantaneous value of the converter grid side voltage. Therefore, in the AC power grid with synchronous generators and non-synchronous generator sources coexisting, the traditional short-circuit current calculation and transient synchronization stability calculation can no longer be accomplished by the electromechanical transient analysis method, so it is predictable that the electromagnetic transient analysis method will finally replace the electromechanical transient analysis method in analyzing the generalized synchronization stability of the power system.

Example to Illustrate the Necessity to Use the Electromagnetic Transient Analysis Method to Analyze the Generalized Synchronization Stability of a Power System

The example system is a two area four machine system [11], with its basic structure as shown in Figure 10, and the relevant parameters can be found in reference [33]. In the original system, G1, G2, G3 and G4 are all synchronous generators with a capacity of 900 MVA. Now the synchronous generator G1 is replaced with a modular multi-level converter (MMC), which has the same capacity as G1 and adopts the power synchronization control. In this way, there are one non-synchronous machine source and three synchronous generator sources in Figure 10. So the synchronization stability of the example system shown in Figure 10 belongs to the category of the generalized synchronization stability. For evaluating the generalized synchronization stability of the example system, the electromechanical transient simulation method is not adequate because it can only give the positive sequence fundamental frequency phasors of the voltage and current; while in simulating the MMC, the instantaneous values of voltage and current must be used.

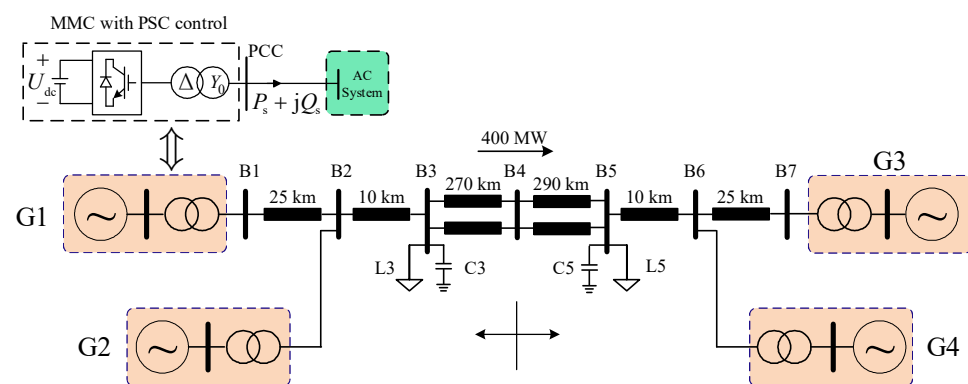


Figure 10. The 2-area 4-machine power system.

Now the electromagnetic transient simulation software PSCAD / EMTDC is used to evaluate the generalized synchronization stability of the example system shown in Figure 10. The steady-state conditions of the system are shown in Table 1. A three-phase short-circuit fault is applied at $t = 2.0$ s on bus B3, and the fault resistance is 0.01Ω .

Table 1. Steady state of the 2-area 4-machine power system.

	States of the Power Sources			
	MMC (G1)	G2	G3	G4
Active power/MW	700	700	719	700
Reactive power/MVar	185.028	234.612	189.838	234.132
Terminal voltage/p.u.	$1.03 \angle 73.02^\circ$	$1.01 \angle 63.25^\circ$	$1.03 \angle 0^\circ$	$1.01 \angle -10.28^\circ$
	Loads and Reactive Power Supplied			
	L3	C3	L5	C5
Active power/MW	967	0	1767	0
Reactive power/MVar	100	-297.917	100	-350

The simulation waveforms are shown in Figure 11 with G3 being the phase angle reference generator [33]. In Figure 11, δ_{13} , δ_{23} and δ_{43} are the voltage phase angle on the high voltage bus of the three power sources MMC, G2 and G4 respectively; P_1 , P_2 , P_3 and P_4 are the active power of the four power sources MMC, G2, G3 and G4 respectively; Q_1 , Q_2 , Q_3 and Q_4 are the reactive power of the four power sources MMC, G2, G3 and G4 respectively; U_1 , U_2 , U_3 and U_4 are the voltage magnitude on the high voltage bus of the four power sources MMC, G2, G3 and G4 respectively; U_{d1} and U_{q1} are the d axis and q axis components of the PCC voltage of the MMC; I_{dref} and I_{qref} (i_{vdq}^*) are the d axis and q axis components of the current reference of the inner control loop of the MMC.

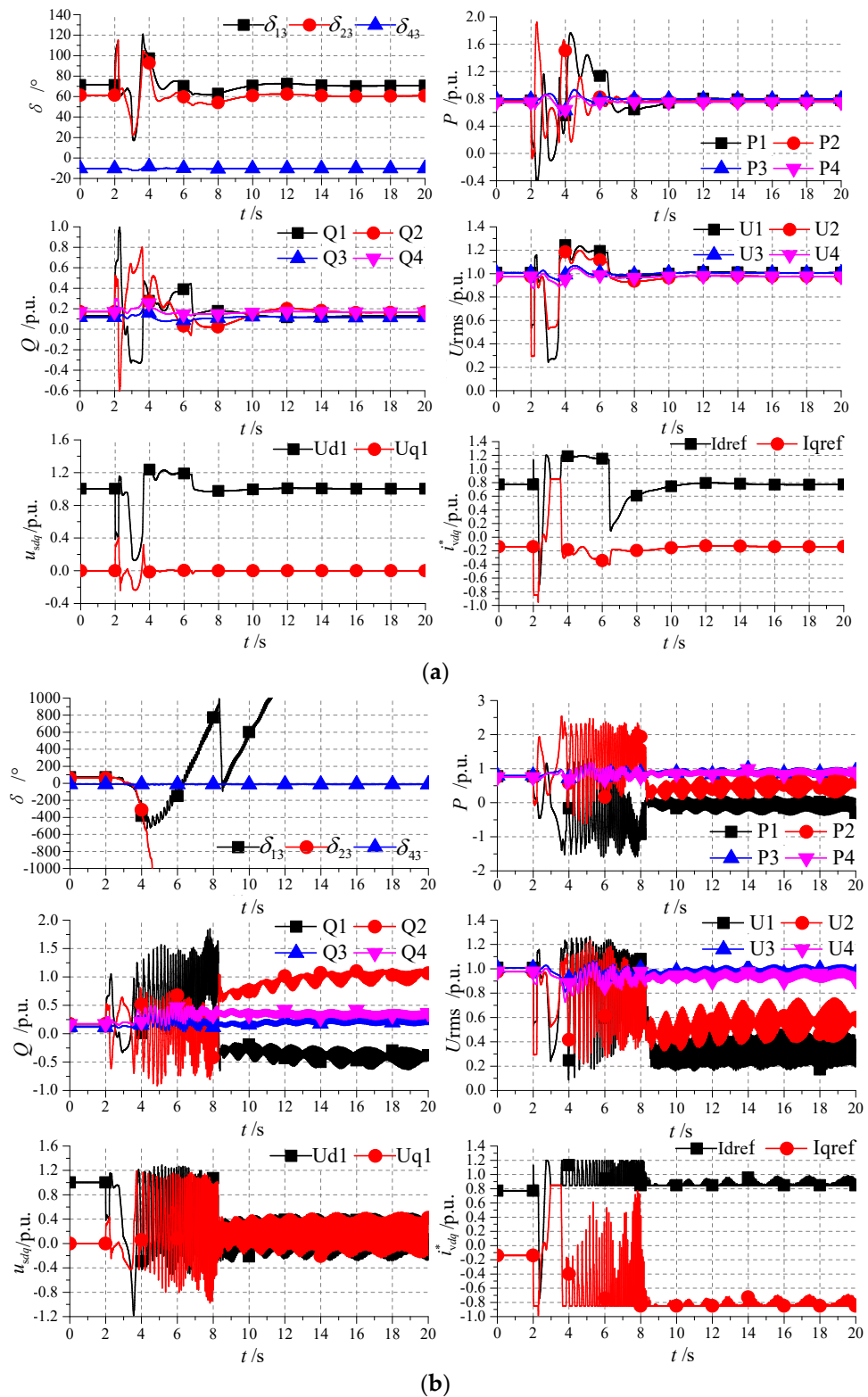


Figure 11. The critical clearing time for three-phase short-circuit fault on B3: (a) The fault duration of 0.198 s; (b) The fault duration of 0.199 s.

In the simulation, the critical clearing time is adopted as an index to evaluate the generalized synchronization stability performance of the system. The meaning of the critical clearing time is: if the fault clearing time is less than the critical clearing time, the system can maintain stable after the fault is cleared; if the fault clearing time is larger than

the critical clearing time, the system can no longer maintain stable after the fault is cleared. So the larger the critical clearing time, the better the generalized synchronization stability of the system. From Figure 11, it can be seen that the critical clearing time for the fault is 0.198 s. When the fault duration is larger than 0.198 s (for example 0.199 s), the system becomes unstable in the sense of the generalized synchronization stability.

7. Analysis Method of Broadband Resonance Instability Caused by Negative Resistance of Power Electronic Devices

When the power system is disturbed, the transmission and distribution network will enter the process of electromagnetic transient oscillation. Besides the forced components of fundamental frequency, the voltage and current responses also contain the free components oscillating at the natural resonance frequencies. In the traditional electromechanical transient analysis, as described in Section 6, those free components are considered to be decayed to zero instantly [32].

The stability of broadband resonance caused by negative resistance of power electronic devices is defined based on the characteristics of the above-mentioned free components oscillating at the natural resonance frequencies. In fact, the transmission and distribution network will enter the process of electromagnetic transient oscillation after being disturbed, and the free components in the voltage and current responses that oscillate at the natural resonance frequencies may not necessarily attenuate, because some power electronic devices connected to the transmission and distribution network may have negative resistance effect in a certain frequency band, just as the synchronous generator will show negative resistance effect in the sub-synchronous frequency band. When the inherent resistance of the power system itself is not enough to offset the negative resistance existing in the power electronic devices, the free components in the voltage and current responses that oscillate at the natural resonance frequencies will not all attenuated; this situation is defined as the resonance instability. Because the distribution of the natural resonance frequencies is extremely wide, the attenuation characteristics of the free components oscillating at the natural resonance frequencies in the voltage and current responses after disturbance is defined as the broadband resonance stability [34]. That is, when all the free components oscillating at the natural resonance frequencies in the voltage and current responses are attenuated, the system is called as resonantly stable, otherwise the system is called as resonantly instable.

In practical engineering, there are many examples of broadband resonance instability. Here are some examples occurred in China. In the period of 2012 to 2017, the interaction between the doubly fed wind farm and its series compensation capacitors caused hundreds of oscillations in the frequency range of 3~10 Hz in Guyuan area, resulting in abnormal vibration of transformers and a large number of wind turbines being cut off [35]; in 2015, subsynchronous oscillations of frequency within 20~40 Hz involving a wind farm with fully rated converter wind turbines frequently occurred in Hami, exciting torsional vibration of the steam turbine shafts of the synchronous generators in a power plant 300 km away from the wind farm [36]; in 2015, the problem of oscillation in sub-synchronous frequency of about 25 Hz occurred in the DC side of the Xiamen MMC-HVDC transmission project [37]; in 2017 a problem of 1270 Hz high frequency oscillation occurred in the AC side of the Luxi back to back MMC-HVDC project [31]; and in 2018 a problem of 1810 Hz and 700 Hz high frequency oscillations occurred in the AC side of Yue back to back MMC-HVDC project [38].

7.1. Difficulties in Studying Broadband Resonance Stability Based on Electromagnetic Transient Simulation Method

When using time-domain simulation methods to study any kind of system stability, there exists a precondition that the initial operating point of the system is a stable operating point, otherwise the system cannot progress to the initial operating point. Therefore, the general approach of studying stability based on the time-domain simulation method is starting from a stable initial operating point of the system, simulating the system in several

time steps, and then changing the structure or parameters of the system or the controllers at different time points to examine the time responses of the system. If the responses of the system oscillate divergently, the system under this disturbance is assessed as instable; and if the system can progress to a new stable operating point over time, the system under this disturbance is assessed as stable.

For a power system containing many power electronic devices, the resonance stability of an initial operating point cannot be determined directly. For a system whose initial operating point itself is resonantly instable, the initial operating state of the system cannot be established through the electromagnetic transient simulation. Therefore, when the electromagnetic transient simulation method is used to study the broadband resonance stability, only the system whose initial operating point is resonantly stable can be studied, while the system whose initial operating point itself is resonantly instable cannot be studied by the electromagnetic transient simulation method. So, for broadband resonance stability analysis, other methods are needed.

7.2. Difficulties in Studying Broadband Resonance Stability Based on State Space Model

The broadband resonance stability problem is aimed at the linearized system of the power system at a certain operating point, which belongs to the category of small signal analysis. Therefore, the grid elements considered are always linear elements. When the power system is composed of lumped parameter components, in the simplest case, assuming that the component parameters do not change with frequency, the power system can be represented by the standard state space model with time-invariant parameters as follows:

$$\dot{\mathbf{X}} = \mathbf{A}\mathbf{X} + \mathbf{B}\mathbf{U} \quad (3)$$

where, \mathbf{X} is the state vector, \mathbf{A} is the state matrix, \mathbf{B} is the control coefficient matrix, \mathbf{U} is the control input vector. In this case, the resonance stability of the power system can be determined directly:

- the eigenvalues of matrix \mathbf{A} are the resonant modes;
- all the eigenvalues of matrix \mathbf{A} are all the resonant modes of the power system;
- if all the eigenvalues of matrix \mathbf{A} are in the left half plane of the complex plane, then the power system is resonantly stable.

And for the power system composed of lumped parameter elements, the number of the resonant modes are finite.

However, there are three main difficulties when using the state space model to study the broadband resonance stability of power systems with many power electronic devices.

- When considering distributed parameter elements such as transmission lines, the equation describing the characteristics of distributed parameter elements is a partial differential equation, so the whole power system cannot be described by the standard state space model of linear time invariant system.
- If we further consider the characteristics of component parameters changing with the frequency, even for a power system composed of lumped parameter components, it cannot be described by the standard state space model of a linear time-invariant system.
- For power electronic devices, it is not easy to establish a linear state space model at a certain operating point.

7.3. Advantages of S-Domain Nodal Admittance Matrix Method in Studying Broadband Resonance Stability

In 1999, reference [39] proposed the method for analyzing the broadband resonance stability of power systems by using s-domain nodal admittance matrix $\mathbf{Y}(s)$. In 2001, reference [40] made further development and improvement on the analysis method of nodal admittance matrix in s-domain.

The main points of analyzing the resonance stability of power system by using s-domain nodal admittance matrix $\mathbf{Y}(s)$ are as follows [34]:

- (1) The so-called s -domain nodal admittance matrix $\mathbf{Y}(s)$ is also called operational admittance matrix $\mathbf{Y}(s)$. For example, the operational admittance of the capacitance C is sC , and that of the inductance L is $1/sL$. In short, replacing $j\omega$ in the element admittance model for AC steady-state analysis with s constitutes the operational admittance of the corresponding element. Similar results are obtained for transmission lines with distributed parameters. After obtaining the operational admittance model of each element, the steps of constructing the operational admittance matrix of the whole system $\mathbf{Y}(s)$ are the same as the steps of constructing the nodal admittance matrix in AC steady-state analysis.
- (2) For a power system containing distributed parameter elements and frequency-varying parameter elements, there is no special difficulty in constructing its s -domain nodal admittance matrix. Therefore, for general power systems, it is universal to analyze the resonance stability based on the s -domain nodal admittance matrix $\mathbf{Y}(s)$.
- (3) Let the determinant of $\mathbf{Y}(s)$ be $\det[\mathbf{Y}(s)]$; then the root of $\det[\mathbf{Y}(s)] = 0$ (also called the zero point of $\det[\mathbf{Y}(s)]$) is the resonant mode of the power system, and all zeros of $\det[\mathbf{Y}(s)]$ are all the resonant modes of the power system. If all zeros of $\det[\mathbf{Y}(s)]$ are located in the left half of the complex plane, then the power system is resonantly stable.

The power system model used to establish the s -domain nodal admittance matrix $\mathbf{Y}(s)$ is shown in Figure 12. The entire power system needs to be transformed into a pure operational impedance (or operational admittance) network. After establishing the s -domain nodal admittance matrix, there are many ways to find the zero point of $\det[\mathbf{Y}(s)]$, such as the Newton-Raphson iterative method [40] and other methods [34]. Because there are infinite resonant modes in the power system with distributed parameter elements, the zero point of $\det[\mathbf{Y}(s)]$ is often searched in the specified frequency band in practical engineering analysis. The number of zeros of $\det[\mathbf{Y}(s)]$ in the analyzed frequency band indicates how many inherent resonance modes exist in the analyzed frequency band. Without losing generality, if the i -th zero point of $\det[\mathbf{Y}(s)]$ is $s_i = -\sigma_i + j\omega_i$, then it is the i -th resonant mode of the power system. For the resonant mode $s_i = -\sigma_i + j\omega_i$, the attenuation factor is σ_i , the resonance frequency is $\omega_i/(2\pi)$, and the mode shape is the right eigenvector of the matrix $\mathbf{Y}(s_i)$ corresponding to the eigenvalue $\lambda_0 = 0$.

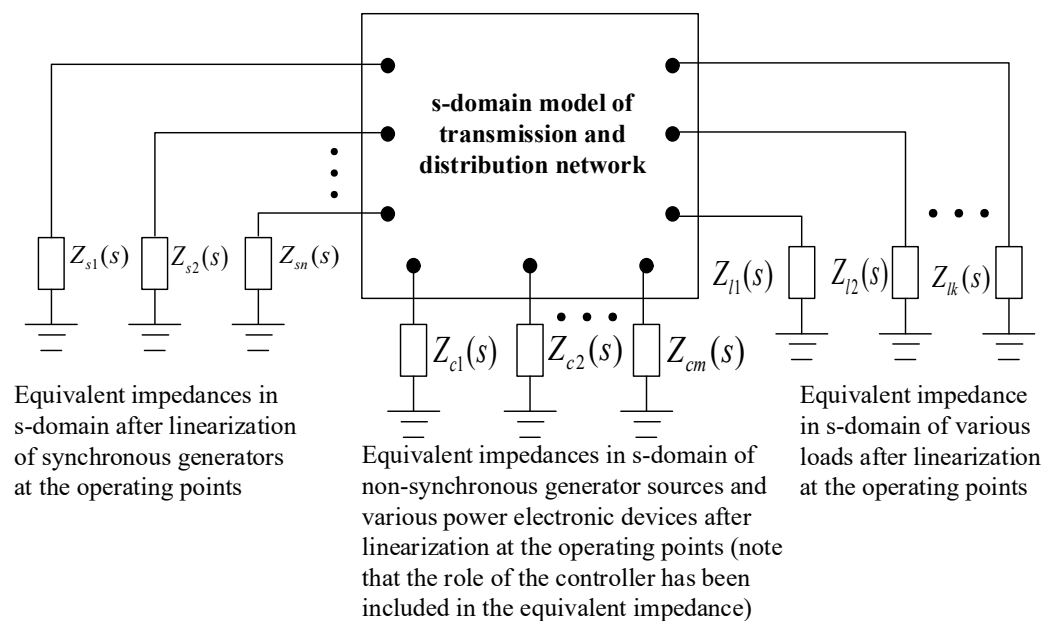


Figure 12. Pure s -domain impedance model of power systems for establishing the s -domain nodal admittance matrix.

7.4. Measures to Improve the Broadband Resonance Stability

For a specific resonant mode s_i , $\mathbf{Y}(s_i)$ is a constant matrix, and $\mathbf{Y}(s_i)$ must have an eigenvalue $\lambda_0 = 0$. The left and right eigenvectors of $\mathbf{Y}(s_i)$ corresponding to the eigenvalue $\lambda_0 = 0$ are calculated to obtain the participation factor of the resonant mode s_i . Obviously, the participation factor indicates the degree to which each node in the power system participates in the resonant mode s_i , so it can be used to locate the main area in the power system participating in the resonant mode s_i . Furthermore, by calculating the sensitivity of the resonant mode $s_i = -\sigma_i + j\omega_i$ with respect to each element y_{ij} in the matrix $\mathbf{Y}(s_i)$, it is possible to determine which system element has a dominant influence on the resonance mode $s_i = -\sigma_i + j\omega_i$. In this way, the specific location and specific device that play a dominant role in the resonant mode $s_i = -\sigma_i + j\omega_i$ can be determined, and the parameter tuning direction of the specific device is also determined. On this basis, there are two control strategies to improve the damping of the resonant mode $s_i = -\sigma_i + j\omega_i$. One strategy is to change the parameters of specific devices to change the impedance frequency characteristics of the existing devices in the power system, such as using virtual impedance control [41–43]; the other strategy is to install new devices to realize the required impedance frequency characteristics [44,45].

7.5. Example to Illustrate the Principle of s-Domain Nodal Admittance Matrix Method

A simplified transmission system is shown in Figure 13, where u_{source} and R_1 are the power source model, R_2 , L_1 , C_1 and C_2 are the transmission line model, and R_3 is the load model. Now we use the state space model and the s-domain nodal admittance matrix method to calculate the natural resonance modes of the system.

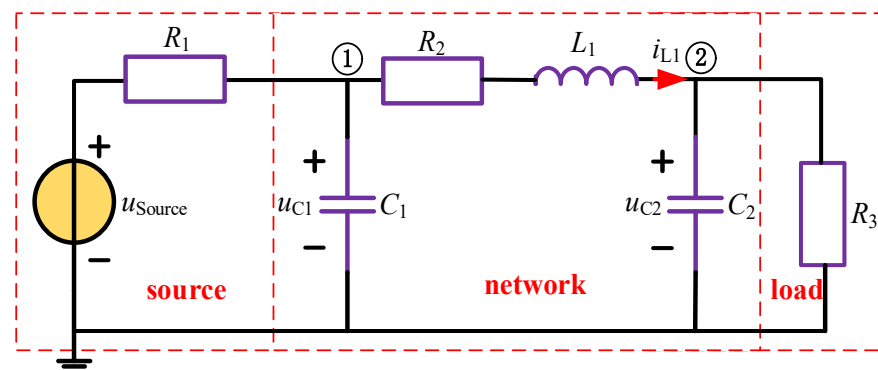


Figure 13. A simplified transmission system diagram.

7.5.1. Calculation Process of the State Space Model

Set the state variables as i_{L1} , u_{C1} and u_{C2} , as shown in Figure 13. According to the mathematical models of the inductor and the capacitor, the state space model of the system shown in Figure 13 can be obtained as shown in Equation (4).

$$\frac{d}{dt} \begin{bmatrix} i_{L1} \\ u_{C1} \\ u_{C2} \end{bmatrix} = \begin{bmatrix} -\frac{R_2}{L_1} & \frac{1}{L_1} & -\frac{1}{L_1} \\ -\frac{1}{C_1} & -\frac{1}{R_1 C_1} & 0 \\ \frac{1}{C_2} & 0 & -\frac{1}{R_3 C_2} \end{bmatrix} \begin{bmatrix} i_{L1} \\ u_{C1} \\ u_{C2} \end{bmatrix} + \begin{bmatrix} 0 \\ \frac{1}{R_1 C_1} \\ 0 \end{bmatrix} u_{\text{source}} \quad (4)$$

according to Equations (3) and (4), we obtain matrix \mathbf{A} as

$$\mathbf{A} = \begin{bmatrix} -\frac{R_2}{L_1} & \frac{1}{L_1} & -\frac{1}{L_1} \\ -\frac{1}{C_1} & -\frac{1}{R_1 C_1} & 0 \\ \frac{1}{C_2} & 0 & -\frac{1}{R_3 C_2} \end{bmatrix} \quad (5)$$

Therefore, the characteristic equation of the system is

$$\det(\lambda I - \mathbf{A}) = \begin{vmatrix} \lambda + \frac{R_2}{L_1} & -\frac{1}{L_1} & \frac{1}{L_1} \\ \frac{1}{C_1} & \lambda + \frac{1}{R_1 C_1} & 0 \\ -\frac{1}{C_2} & 0 & \lambda + \frac{1}{R_3 C_2} \end{vmatrix} = 0 \quad (6)$$

Expanding Equation (6), we obtain

$$\det(\lambda I - \mathbf{A}) = \left(\begin{aligned} & \lambda^3 + \lambda^2 \left(\frac{R_2}{L_1} + \frac{1}{R_1 C_1} + \frac{1}{R_3 C_2} \right) + \\ & + \lambda \left(\frac{1}{L_1 C_2} + \frac{1}{L_1 C_1} + \frac{1}{R_1 R_3 C_1 C_2} + \frac{R_2}{R_1 L_1 C_1} + \frac{R_2}{R_3 L_1 C_2} \right) + \\ & + \frac{1}{R_1 L_1 C_1 C_2} + \frac{1}{R_3 L_1 C_1 C_2} + \frac{R_2}{R_1 R_3 L_1 C_1 C_2} \end{aligned} \right) = 0 \quad (7)$$

7.5.2. Calculation Process of the s-Domain Nodal Admittance Matrix Method

The s-domain nodal admittance matrix of the system shown in Figure 13 is shown in Equation (8),

$$\mathbf{Y}(s) = \begin{bmatrix} \frac{1}{R_1} + \frac{1}{R_2 + sL_1} + sC_1 & -\frac{1}{R_2 + sL_1} \\ -\frac{1}{R_2 + sL_1} & \frac{1}{R_2 + sL_1} + \frac{1}{R_3} + sC_2 \end{bmatrix} \quad (8)$$

Now we calculate the roots of $\det(\mathbf{Y}(s)) = 0$,

$$\det(\mathbf{Y}(s)) = \begin{vmatrix} \frac{1}{R_1} + \frac{1}{R_2 + sL_1} + sC_1 & -\frac{1}{R_2 + sL_1} \\ -\frac{1}{R_2 + sL_1} & \frac{1}{R_2 + sL_1} + \frac{1}{R_3} + sC_2 \end{vmatrix} = 0 \quad (9)$$

Expanding Equation (9), we obtain

$$\det(\mathbf{Y}(s)) = \frac{1}{R_2 + sL_1} \frac{1}{L_1 C_1 C_2} \left(\begin{aligned} & s^3 + s^2 \left(\frac{R_2}{L_1} + \frac{1}{R_1 C_1} + \frac{1}{R_3 C_2} \right) + \\ & + s \left(\frac{1}{L_1 C_2} + \frac{1}{L_1 C_1} + \frac{1}{R_1 R_3 C_1 C_2} + \frac{R_2}{R_1 L_1 C_1} + \frac{R_2}{R_3 L_1 C_2} \right) + \\ & + \frac{1}{R_1 L_1 C_1 C_2} + \frac{1}{R_3 L_1 C_1 C_2} + \frac{R_2}{R_1 R_3 L_1 C_1 C_2} \end{aligned} \right) = 0 \quad (10)$$

By comparing Equations (7) and (10), we can see that they have the same roots, that is, the natural resonance modes of the system calculated by the state space model is identical to that calculated by the s-domain nodal admittance matrix method. However, the s-domain nodal admittance matrix method is much stronger in its applicability. The advantages of the s-domain nodal admittance matrix method compared with the state space model have been described in Sections 7.2 and 7.3.

7.6. Application Example of the s-Domain Nodal Admittance Matrix Method in Real Engineering

As mentioned in the previous section, in 2015, subsynchronous power oscillations of frequency of 20~40 Hz involving a wind farm with fully rated converter wind turbines frequently occurred in Hami of Xinjiang, China. This phenomenon can be analyzed by the s-domain nodal admittance matrix method. Here are some results of the analysis [46].

There are sixteen wind farms composed of fully rated converter wind generators, whose total capacity are 1200 MW. The transmission network of the wind power base is shown in Figure 14, and the relevant parameters can be found in reference [46].

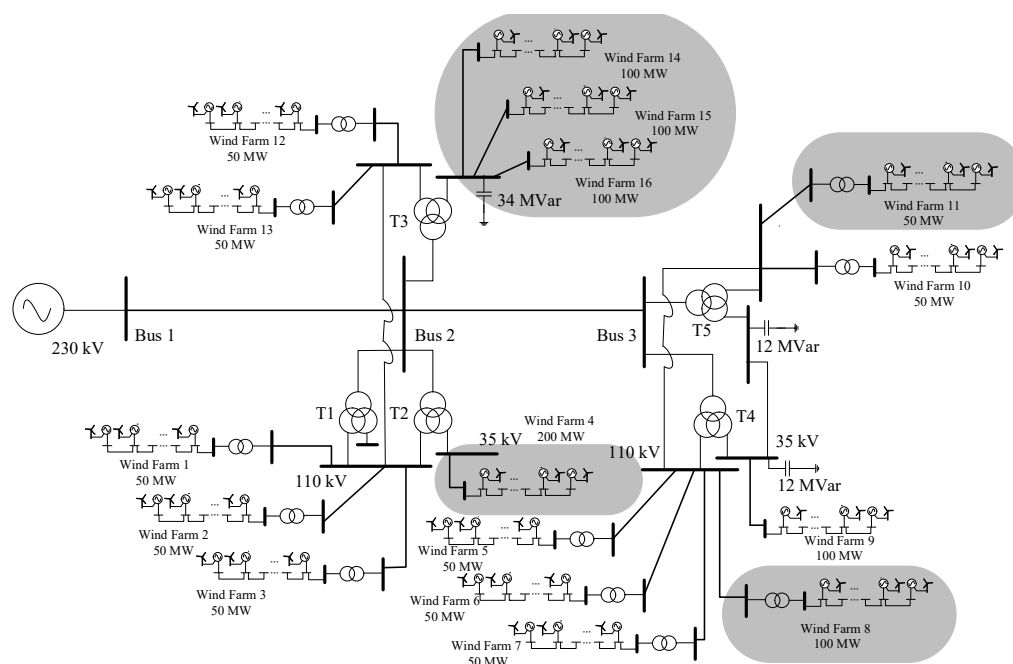


Figure 14. Schematic Structure Diagram of the Wind Power Base.

By using the s-domain nodal admittance matrix method, the resonance modes below 100 Hz are listed in Table 2. It can be seen that the 77.1 Hz resonance mode is instable, and it has been verified that this instable resonance mode is the cause of the subsynchronous power oscillations of frequency of 20~40 Hz [46].

Table 2. The resonance modes below 100 Hz in the Wind Power Base.

Mode	Attenuation Factor/s ⁻¹	Resonance Frequency/Hz
1	2.5518	55.7
2	-7.5602	77.1

8. Summary

Based on the basic principles of AC power grid operation, this paper describes three technical challenges faced by the power system in transition. The main conclusions including:

In the AC power grid with synchronous generators and non-synchronous generator sources coexisting, the concept of synchronization stability between synchronous generators should be extended to the concept of generalized synchronization stability to cover the operating condition that all sources with different synchronization mechanisms in the grid must operate in the same frequency.

The non-synchronous generator sources must rely on the control means to realize their synchronization with other power sources in the power grid, and that the decisive factors are the phase-locked loop (PLL) or the power synchronization loop (PSL). The out-of-step in the sense of generalized synchronization stability can be divided into three types, that is, loss of power angle stability between synchronous generators (power angle out-of-step); phase-locking failure of PLL and out-of-step of PSL of non-synchronous generator sources; and out-of-step caused by long time delay of control systems in non-synchronous generator sources.

The electromechanical transient simulation software can only be used to analyze the power angle stability between generators under the assumption that the performance of PLL and PSL is ideal (there is no phase-locking failure of PLL and out-of-step of PSL) and the AC fault is symmetrical, while it cannot be used for analyzing the generalized synchronization stability of general power systems.

With the increasing proportion of non-synchronous generator sources in the power grid, it will be an inevitable trend to use full electromagnetic transient simulation to analyze the generalized synchronization stability of general power systems. This is a very heavy task. The industry is not ready for the change and needs to pay special attention to the change.

After being disturbed, the power transmission and distribution network will enter the process of electromagnetic transient oscillation. The free components in the voltage and current responses that oscillate at the natural resonance frequencies may not necessarily attenuate. The broadband resonance stability describes the attenuation characteristics of those free components oscillating at natural resonance frequencies.

When using electromagnetic transient simulation method to study the broadband resonance stability, we can only study the system whose initial operating point is resonantly stable, but not the system whose initial operating point is resonantly instable.

When the standard state space model is used to study the broadband resonance stability, it is difficult to simulate the distributed parameter elements, frequency dependent elements and power electronic devices.

The s-domain nodal admittance matrix method has great advantages in analyzing and solving the problem of the broadband resonance stability, but it needs first to obtain the characteristic of impedance varying with frequency of the related device.

Funding: This research received no external funding.

Institutional Review Board Statement: Not applicable.

Informed Consent Statement: Not applicable.

Data Availability Statement: Data available on request due to privacy.

Conflicts of Interest: The author declares no conflict of interest.

Abbreviations

Abbreviations	Meaning
DFIG	Doubly Fed Induction Generator
LCC	Line Commutated Converter
MMC	Modular Multilevel Converter
PCC	Point of Common Coupling
PI	Proportional Integral Controller
PLL	Phase Locked Loop
PSC	Power Synchronization Control
PSL	Power Synchronization Loop
pu	per unit
SRF-PLL	Synchronous Reference Frame-Phase Locked Loop
VSC	Voltage Source Converter
VSG	Virtual Synchronous Generator
Symbols	Meaning
A	State matrix in state space model
B	Control coefficient matrix in state space model
dq	Coordinate system rotating in the positive direction (counterclockwise) in grid angular frequency ω
D	Damping coefficient in the motion equation of a generator
H	Generator inertia time constant
i	General symbol for instantaneous value of current
$i_{va}, i_{vb}, i_{vc}, i_{vabc}$	AC phase current at the valve side of a converter
$i_{vd}, i_{vq}, i_{vdq} \dots$	d-axis component and q-axis component of three-phase AC current at the valve side of a converter
L	General symbol for inductance

Abbreviations	Meaning
P	General symbol for fundamental active power or average power
P_e	Electromagnetic power output by a generator
P_m	Mechanical power transmitted to the generator rotor
P_s	Fundamental active power injected into the AC power grid from the AC bus of a converter
P_{sref}	Reference value of fundamental active power injected into the AC power grid from the AC bus of a converter
Q	General symbol for fundamental reactive power
Q_s	Fundamental reactive power injected into the AC power grid from the AC bus of a converter
R	General symbol for resistance
$s_i = -\sigma_i + j\omega_i$	i -th zero point of $\det [Y(s)]$, also called the i -th resonance mode
t	time
$u_{sa}, u_{sb}, u_{sc}, u_{sabc}$	Phase voltage of AC bus of a converter
$u_{sd}, u_{sq}, u_{sdq} \dots$	d-axis and q-axis components of three-phase voltage at the AC bus of a converter station
$u_{s\alpha}, u_{s\beta}$	α -axis and β -axis components of three-phase voltage at the AC bus of a converter station
u_{va}, u_{vb}, u_{vc}	AC phase voltage at the valve side of a converter
U	The control vector in state space model
U_{dc}	DC component of voltage at the DC side of a converter
U_s	Effective value of the AC bus voltage of a converter
X	General symbol for reactance
X	The state vector in state space model
$Y(s)$	s-domain nodal admittance matrix
δ	General symbol for phase angle
θ	Phase angle of phase-a fundamental voltage u_{sa} in cosine form; electrical angle of the generator rotor
λ	Characteristic root in state space model
ω	Angular frequency of the power grid
ω_0	Rated angular frequency of the power grid
$\Delta\omega$	The generator speed deviation
*	The superscript means reference value

References

- Mostafaeipour, A.; Bidokhti, A.; Fakhzad, M.B.; Sadeghieh, A.; Mehrjerdi, Y.Z. A new model for the use of renewable electricity to reduce carbon dioxide emissions. *Energy* **2022**, *238*, 121602. [CrossRef]
- IEA. Renewables 2021 Analysis and Forecast to 2026. Available online: <https://www.iea.org/reports/renewables-2021> (accessed on 1 January 2022).
- O’Sullivan, J.; Rogers, A.; Flynn, D.; Smith, P.; Mullane, A.; O’Malley, M. Studying the maximum instantaneous non-synchronous generation in an island system—Frequency stability challenges in Ireland. *Energy* **2014**, *29*, 2943–2951. [CrossRef]
- Duer, S.; Zajkowski, K.; Harničárová, M.; Charun, H.; Bernatowicz, D. Examination of Multivalent Diagnoses Developed by a Diagnostic Program with an Artificial Neural Network for Devices in the Electric Hybrid Power Supply System “House on Water”. *Energies* **2021**, *14*, 2153. [CrossRef]
- Duer, S.; Valicek, J.; Paš, J.; Stawowy, M.; Bernatowicz, D.; Duer, R.; Walczak, M. Neural Networks in the Diagnostics Process of Low-Power Solar Plant Devices. *Energies* **2021**, *14*, 2719. [CrossRef]
- Seneviratne, C.; Ozansoy, C. Frequency response due to a large generator loss with the increasing penetration of wind/PV generation—A literature review. *Renew. Sustain. Energy Rev.* **2016**, *57*, 659–668. [CrossRef]
- Liu, Y.; You, S.; Tan, J.; Zhang, Y.; Liu, Y. Frequency response assessment and enhancement of the U.S. power grids toward extra-high photovoltaic generation penetrations—An industry perspective. *IEEE Trans. Power Syst.* **2018**, *33*, 3438–3449. [CrossRef]
- Duer, S. Assessment of the Operation Process of Wind Power Plant’s Equipment with the Use of an Artificial Neural Network. *Energies* **2020**, *13*, 2437. [CrossRef]
- Zhou, X.; Chen, S.; Lu, Z.; Huang, Y.; Ma, S.; Zhao, Q. Technology Features of the New Generation Power System in China. *Proc. CSEE* **2018**, *38*, 1893–1904.
- Xue, Y.; Wang, G.; Zhang, Z.; Xu, Z. Mechanism analysis and mitigation strategies for oscillatory instability of synchronous generators affected by voltage source converters. *IET Gener. Transm. Distrib.* **2021**, *16*, 750–765. [CrossRef]
- Kundur, P. *Power System Stability and Control*; McGraw-Hill Incorporated Press: New York, NY, USA, 1994; ISBN 978-007-035-958-1.
- Xu, Z. Physical mechanism and research approach of generalized synchronous stability for power systems. *Electr. Power Autom. Equip.* **2020**, *40*, 3–9. [CrossRef]

13. Xu, Z. Three Technical Challenges Faced by Power Grids with High Proportion of Non-Synchronous Machine Sources. *South. Power Syst. Technol.* **2020**, *14*, 1–9. [[CrossRef](#)]
14. Ortjohan, E.; Arias, A.; Morton, D.; Mohd, A.; Omari, O. Grid-forming three-phase inverters for unbalanced loads in hybrid power systems. In Proceedings of the 4th IEEE World Conference on Photovoltaic Energy Conference, Waikoloa, HI, USA, 5–12 May 2006; IEEE: New York, NY, USA, 2006; pp. 2396–2399.
15. Rocabert, J.; Luna, A.; Blaabjerg, F.; Rodriguez, P. Control of power converters in AC microgrids. *IEEE Trans. Power Electron.* **2012**, *27*, 4734–4749. [[CrossRef](#)]
16. Xu, Z.; Xiao, H.; Zhang, Z.; Xue, Y.; Liu, G.; Tang, G.; Xu, F.; Wang, S.; Tu, Q.; Guan, M.; et al. *Modular Multilevel Converter-Based High Voltage DC Power Transmission Systems*, 2nd ed.; China Machine Press: Beijing, China, 2017; ISBN 978-7-111-55336-6. (In Chinese)
17. Kimbark, E.W. *Direct Current Transmission*; Wiley Interscience Press: Oxford, UK, 1971; ISBN 0-471-47580-7.
18. Anaya-Lara, O.; Jenkins, N.; Ekanayake, J.; Mike, P. *Wind Energy Generation—Modelling and Control*; John Wiley & Sons Press: Hoboken, NJ, USA, 2009; ISBN 978-0-470-71433-1.
19. Blaabjerg, F.; Teodorescu, R.; Liserre, M.; Timbus, A.V. Overview of control and grid synchronization for distributed power generation systems. *IEEE Trans. Ind. Electron.* **2006**, *53*, 1398–1409. [[CrossRef](#)]
20. Zhou, J.; Ding, H.; Fan, S.; Zhang, Y.; Gole, A.M. Impact of short-circuit ratio and phase-locked-loop parameters on the small-signal behavior. *IEEE Trans. Power Deliv.* **2014**, *29*, 2287–2296. [[CrossRef](#)]
21. Florian, H.; Walter, S.; Lennart, H. Small-Signal Modeling of Three-Phase Synchronous Reference Frame Phase-Locked Loops. *IEEE Trans. Power Electron.* **2018**, *33*, 5556–5560. [[CrossRef](#)]
22. Rodríguez, P.; Pou, J.; Bergas, J.; Candela, J.I.; Burgos, R.P.; Boroyevich, D. Decoupled double synchronous reference frame PLL for power converters control. *IEEE Trans. Power Electron.* **2007**, *22*, 584–592. [[CrossRef](#)]
23. Kaura, V.; Blasco, V. Operation of a phase locked loop system under distorted utility conditions. *IEEE Trans. Ind. Appl.* **1997**, *33*, 58–63. [[CrossRef](#)]
24. Chung, S. A phase tracking system for three phase utility interface inverters. *IEEE Trans. Power Electron.* **2000**, *15*, 431–438. [[CrossRef](#)]
25. Zhang, L.; Harnefors, L.; Nee, H. Power-synchronization control of grid-connected voltage-source converters. *IEEE Trans. Power Syst.* **2010**, *25*, 809–820. [[CrossRef](#)]
26. Beck, H.; Hesse, R. Virtual Synchronous Machine. In Proceedings of the 9th International Conference on Electrical Power Quality and Utilization, Barcelona, Spain, 9–11 October 2007; IEEE: New York, NY, USA, 2007; pp. 1–6.
27. Guan, M.; Pan, W.; Zhang, J.; Hao, Q.; Cheng, J.; Zheng, X. Synchronous Generator Emulation Control Strategy for Voltage Source Converter (VSC) Stations. *IEEE Trans. Power Syst.* **2015**, *30*, 3093–3101. [[CrossRef](#)]
28. Anderson, P.; Fouad, A. *Power System Control and Stability*, 2nd ed.; John Wiley & Sons Press: Hoboken, NJ, USA, 2002; ISBN 0-471-23862-7.
29. Wu, H.; Wang, X. Design-Oriented Transient Stability Analysis of Grid-Connected Converters with Power Synchronization Control. *IEEE Trans. Ind. Electron.* **2019**, *66*, 6473–6482. [[CrossRef](#)]
30. Taul, M.; Wang, X.; Davari, P.; Blaabjerg, F. An Overview of Assessment Methods for Synchronization Stability of Grid-Connected Converters Under Severe Symmetrical Grid Faults. *IEEE Trans. Power Electron.* **2019**, *34*, 9655–9670. [[CrossRef](#)]
31. Zou, C.; Rao, H.; Xu, S.; Li, Y.; Li, W.; Chen, J.; Zhao, X.; Yang, Y.; Lei, B. Analysis of Resonance between a VSC-HVDC Converter and the AC Grid. *IEEE Trans. Power Electron.* **2018**, *33*, 10157–10168. [[CrossRef](#)]
32. Xu, Z. *Dynamic Performance Analysis of AC/DC Power Systems*; China Machine Press: Beijing, China, 2004; ISBN 7-111-14294-2. (In Chinese)
33. Wang, Y.; Zhou, Y.; Zhou, K.; Wang, T.; Xu, Z.; Li, X. Study on Transient Stability of Power System Containing Non-Synchronous Machine Sources Based on PSCAD/EMTDC. In Proceedings of the 4th International Conference on HVDC, Xi’an, China, 6–9 November 2020; IEEE: New York, NY, USA, 2020; pp. 276–281.
34. Xu, Z.; Wang, S.; Xing, F. Study on the Method for Analyzing Electric Network Resonance Stability. *Energies* **2018**, *11*, 646. [[CrossRef](#)]
35. Wang, L.; Xie, X.; Jiang, Q.; Liu, H.; Li, Y.; Liu, H. Investigation of SSR in practical DFIG-based wind farms connected to a series compensated power system. *IEEE Trans. Power Syst.* **2014**, *30*, 2772–2779. [[CrossRef](#)]
36. Liu, H.; Xie, X.; He, J.; Xu, T.; Yu, Z.; Wang, C.; Zhang, C. Subsynchronous interaction between direct-drive PMSG based wind farms and weak AC networks. *IEEE Trans. Power Syst.* **2017**, *32*, 4708–4720. [[CrossRef](#)]
37. Li, Y.; Tang, G.; He, Z.; An, T.; Yang, J.; Wu, Y.; Kong, M. Damping Control Strategy Research for MMC Based HVDC System. *Proc. CSEE* **2016**, *36*, 5492–5503. [[CrossRef](#)]
38. Guo, X.; Liu, B.; Mei, H. Analysis and suppression of resonance between AC and DC systems in Chongqing-Hubei Back-to-Back HVDC Project of China. *Autom. Electr. Power Syst.* **2020**, *44*, 157–164. [[CrossRef](#)]
39. Semlyen, A. s-Domain methodology for assessing the small signal stability of complex systems in non-sinusoidal steady state. *IEEE Trans. Power Syst.* **1999**, *14*, 132–137. [[CrossRef](#)]
40. Gomes, S.; Martins, N.; Portela, C. Modal analysis applied to s-domain models of ac networks. In Proceedings of the 2001 IEEE/PES Winter Meeting, Columbus, OH, USA, 28 January–1 February 2001; IEEE: New York, NY, USA, 2001; pp. 1305–1310.

41. He, J.; Li, Y. Analysis, Design, and Implementation of Virtual Impedance for Power Electronics Interfaced Distributed Generation. *IEEE Trans. Ind. Appl.* **2011**, *47*, 2525–2538. [[CrossRef](#)]
42. He, J.; Li, Y. Generalized Closed-Loop Control Schemes with Embedded Virtual Impedances for Voltage Source Converters with LC or LCL Filters. *IEEE Trans. Power Electron.* **2012**, *27*, 1850–1861. [[CrossRef](#)]
43. Zhong, Q.; Zeng, Y. Control of Inverters Via a Virtual Capacitor to Achieve Capacitive Output Impedance. *IEEE Trans. Power Electron.* **2014**, *29*, 5568–5578. [[CrossRef](#)]
44. Zhang, Y.; Yang, Y.; Chen, X.; Gong, C. Intelligent Parameter Design-Based Impedance Optimization of STATCOM to Mitigate Resonance in Wind Farms. *IEEE J. Emerg. Sel. Top. Power Electron.* **2021**, *9*, 3201–3215. [[CrossRef](#)]
45. Zhang, Y.; Wang, Y.; Zhang, D.; Chen, X.; Gong, C. Broadband Impedance Shaping Control Scheme of MMC-Based STATCOM for Improving the Stability of the Wind Farm. *IEEE Trans. Power Electron.* **2021**, *36*, 10278–10292. [[CrossRef](#)]
46. Xing, F.; Xu, Z.; Zhang, Z.; Dan, Y.; Zhu, Y. Resonance Stability Analysis of Large-Scale Wind Power Bases with Type-IV Wind Generators. *Energies* **2020**, *13*, 5220. [[CrossRef](#)]